Analysis of a New Compact Microstrip Antenna

Jacob George, C. K. Aanandan, P. Mohanan, and K. G. Nair

***Abstract*—A new compact microstrip antenna element is analyzed. The analysis can accurately predict the resonant frequency, input impedance, and radiation patterns. The predicted results are compared with experimental results and excellent agreement is observed. These antenna elements are more suitable in applications where limited antenna real estate is available.**

***Index Terms*—Microstrip antennas.**

I. Introduction

MICROSTRIP antennas are popular and are getting increased attention due to their excellent advantages. Depending upon the application, microstrip antennas having different geometrical shapes are used [1]. Nowadays, researchers are interested in the design and development of compact microstrip radiating elements [2]–[6]. Recently, the authors have experimentally demonstrated the development of such a new compact microstrip antenna [7]. The proposed antenna does not have a regular geometric shape and, hence, analytical techniques such as transmission-line model [8] and cavity model [9] cannot be used directly. However, popular numerical techniques like finite-element method, finite-difference time-domain (FDTD) methods, etc., could be used for the analysis [10], [11]. Here a computationally efficient method is adopted since the geometry of the proposed antenna could be readily divided into few regular and simple geometric shapes with much less effort.

In this paper, the generalized cavity model [12] and the spatial Fourier transform technique [13] are suitably modified for the analysis of the proposed compact antenna configurations. The analysis can accurately predict the resonant frequency, input impedance, and radiation patterns. The method is validated through comparison with experimental results.

The magnetic wall model of the patch is developed by replacing the fringing fields at the periphery by outward equivalent edge extensions equal to the height of the substrate. The top metallization of the patch with magnetic wall model is shown in Fig. 2(a). The feed point is specified in terms of the coordinates (X_0, Y_0).

II. Analysis

The geometry of the new compact antenna with the coordinate system is shown in Fig. 1. The radiating patch is etched on a substrate of dielectric constant ε_r and thickness h.

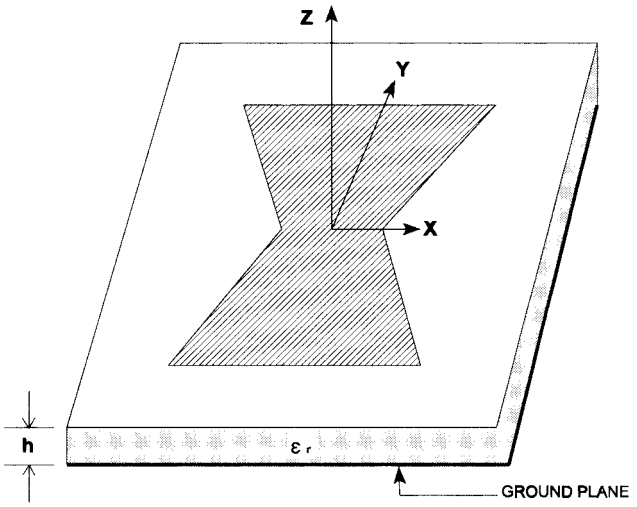

Fig. 1. Geometry of the proposed compact microstrip antenna with coordinate system.

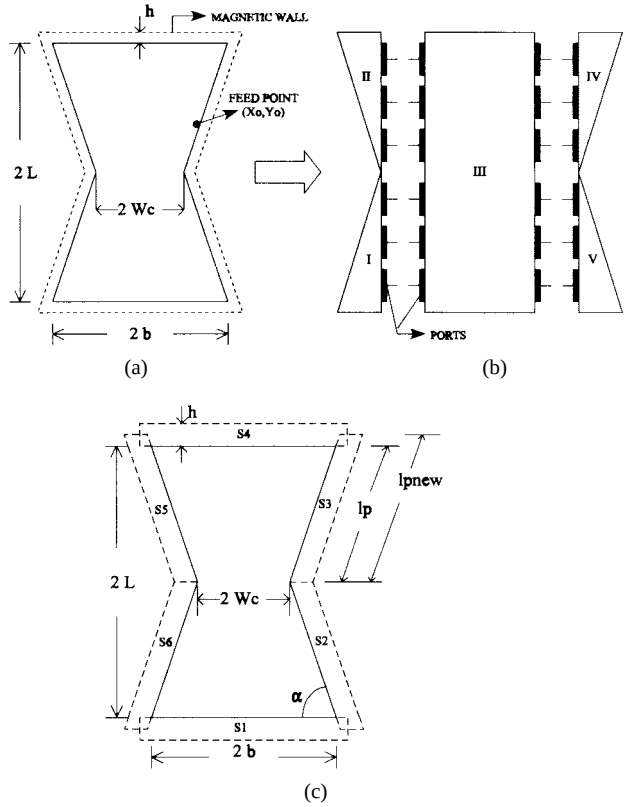

Fig. 2. (a) Top metallization of the compact antenna showing various physical dimensions and magnetic wall model. (b) Segmentation of the equivalent geometry shown in (a) in terms of triangular and rectangular shapes. (c) Aperture model of the antenna with six radiating slots (S1, S2, $\cdots$, S6).

The equivalent geometry obtained after giving edge extensions is then divided into different segments [I, II, III, IV, and

Manuscript received October 13, 1997; revised May 10, 1998. The work of J. George was supported by the Council of Scientific and Industrial Research (CSIR), Government of India.

The authors are with the Department of Electronics, Cochin University of Science and Technology, Cochin 682 022, Kerala, India.

Publisher Item Identifier S 0018-926X(98)08894-2.

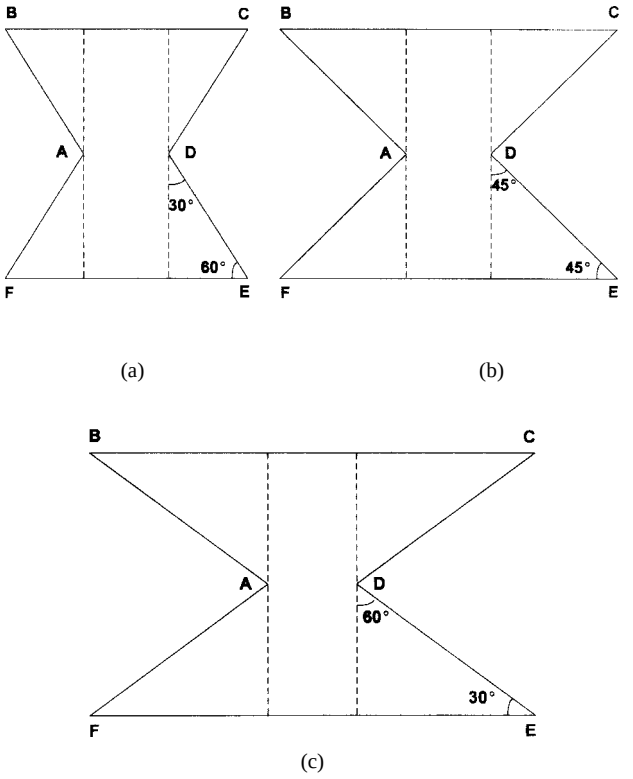

Fig. 3. The three antenna configurations used for the analysis. (a) Antenna A ($\varepsilon_r = 4.5$, $h = 0.16$ cm, $W_c = 1$ cm, $b = 3.0$ cm, $L = 3.4641$ cm, $\angle\alpha = 60°$, $X_0 = 1.50$ cm, $Y_0 = 0.87$ cm). (b) Antenna B ($\varepsilon_r = 4.5$, $h = 0.16$ cm, $W_c = 1$ cm, $b = 4.4641$ cm, $L = 3.4641$ cm, $\angle\alpha = 45°$, $X_0 = 1.92$ cm, $Y_0 = 0.92$ cm). (c) Antenna C ($\varepsilon_r = 6$, $h = 0.065$ cm, $W_c = 1$ cm, $b = 7.0$ cm, $L = 3.4641$ cm, $\angle\alpha = 30°$, $X_0 = 2.30$ cm, $Y_0 = 0.75$ cm).

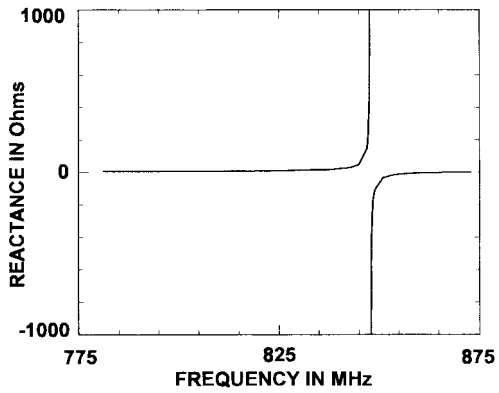

Fig. 4. Variation of input reactance with frequency for the antenna A.

V as given in Fig. 2(b)] of rectangular and triangular shapes for which Green's functions are available [14], [15]. As the Green's functions of 30°–60°–90° and 45°–45°–90° triangles are available, mainly three-symmetric antenna configurations, as shown in Fig. 3, are analyzed here. The theory can be extended to other configurations as well.

The different segments are assumed to be connected at a number of interconnection points only. The total interconnection length is divided into a number of ports (port width $\leq \lambda_g/20$, λ_g is the intrinsic wavelength in the patch) and the interconnection points are associated with ports as shown

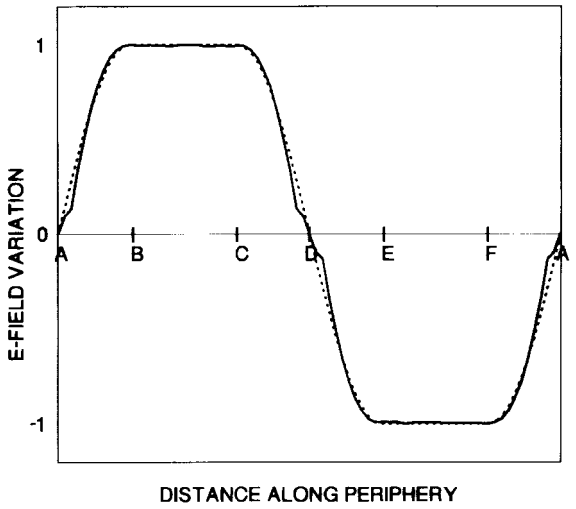

Fig. 5. Variation of normalized electric field along the periphery of antenna A for the TM_{01} mode computed. – – – – – cosine field variations (along AB, CD, DE, and FA) and ——— constant field (along BC and EF).

in Fig. 2(b). The segments are treated as multiport planar networks and the Z matrix of them are evaluated as [16]

$$Z_{ij}^{s} = \frac{1}{W_i W_j} \int_{PW_i} \int_{PW_j} G^{s}(s/s_0)\, ds\, ds_0 \qquad (1)$$

where Z_{ij}^{s} is the i, jth element of the Z matrix of the segment, and W_i, W_j and PW_i, PW_j are the effective and physical widths of the ith and jth ports. The Green's function G^S depends on the shape of the segment.

For the rectangular and triangular segment, (1) is evaluated by using the Green's functions as given in [16].

Now multiport connection method [16] is used to combine the Z matrices of the individual segments to get the overall Z matrix and, hence, the input reactance of the lossless cavity under the patch (neglecting the radiation, conductor, dielectric, and surface wave losses). Fig. 4 shows the typical variation of input reactance with frequency for the structure shown in Fig. 3(a). An extremely large value of the input reactance indicates resonance [12]. A similar variation is observed for the other antennas shown in Fig. 3. The theoretical resonance frequencies obtained for the three antennas A, B, and C are 848, 695, and 468 MHz, respectively. The corresponding experimental values are 828, 706, and 477 MHz. In all the above cases, the patch area is less than 35% of a conventional rectangular microstrip antenna fabricated on the same substrate and resonating at the same frequency. The patch area of antenna A is 24.25 cm^2, whereas the area of the corresponding rectangular patch is 88.77 cm^2.

To get the actual input impedance variation, the energy lost should be incorporated as an effective loss tangent δ_{eff} [9]. The effective loss tangent modifies the dielectric constant to a complex value, which, in turn, modifies the wave number to an effective value, k_{eff}. The modified wave number will be used for the evaluation of Green's function of the segments and the overall impedance matrix is evaluated once again to obtain the actual input impedance.

To get the radiation pattern and the effective loss tangent, the Z-directed electric field distribution in the patch is to be

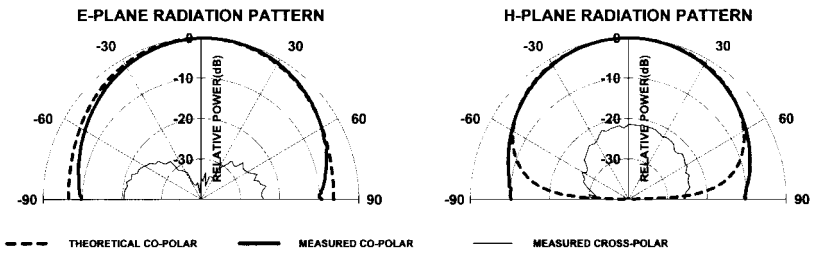

Fig. 6. Theoretical and experimental E-plane and H-plane radiation patterns of the antenna A.

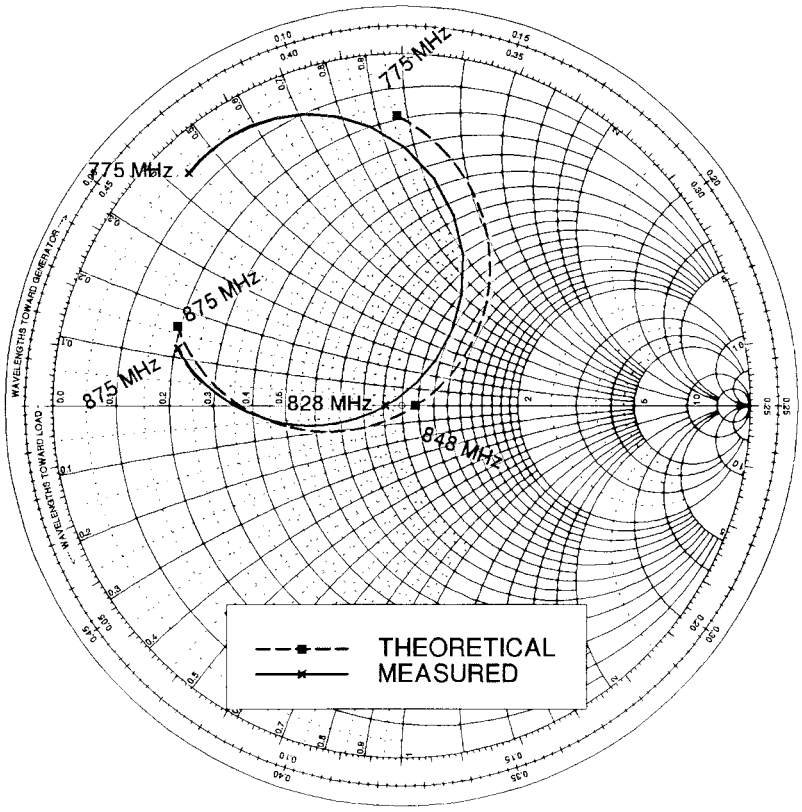

(a)

Fig. 7. Theoretical and experimental impedance loci of the antennas A, B, and C. (a) Antenna A.

determined. The Z-directed electric field in a segment is given by [12]

$$E_z^s = \hat{z}\frac{1}{h}\int G^s(s/s_0)J_s(s_0)\,ds_0. \tag{2}$$

$J_s(s_0)$ is the continuous current density at the interconnection between segments. It is obtained from the RF port currents as given in [17]. The port currents are determined from the impedance matrix elements of different segments [12]. Fig. 5 shows the computed electric field variation (normalized) along the periphery of the antenna A. Similar variations are observed for the other two antennas. From these field variations the mode is identified as TM_{01}. For the evaluation of radiation patterns, the curves of computed electric field variation along the periphery in Fig. 5 are assumed (also shown in Fig. 5) to be cosine quarter wave along the hypotenuse of the triangular segments and constant fields along all other sides (sides of the segments constituting the periphery of the antenna). From Fig. 5, it is found that the assumed and the computed electric field variations along the periphary closely resembles and the former is used as aperture excitations for the computation of the radiation pattern.

Aperture model [13] of the antennas are constructed by putting six radiating aperture slots (S1, S2, $\cdots$, S6) along the periphery of the antenna as given in Fig. 2(c). The slots are assumed to be having a width equal to the dielectric thickness (h).

For all the above antenna configurations (A, B, and C), the aperture excitation field E_1 corresponding to slot S1 is given by

$$E_1 = E_0\cos\left[\frac{m\pi\left(b+\frac{h}{2}+x\right)}{2\left(b+\frac{h}{2}\right)}\right] \qquad -\left(b+\frac{h}{2}\right)\le x\le\left(b+\frac{h}{2}\right). \tag{3}$$

A similar expression with appropriate limits can be used for slot S4.

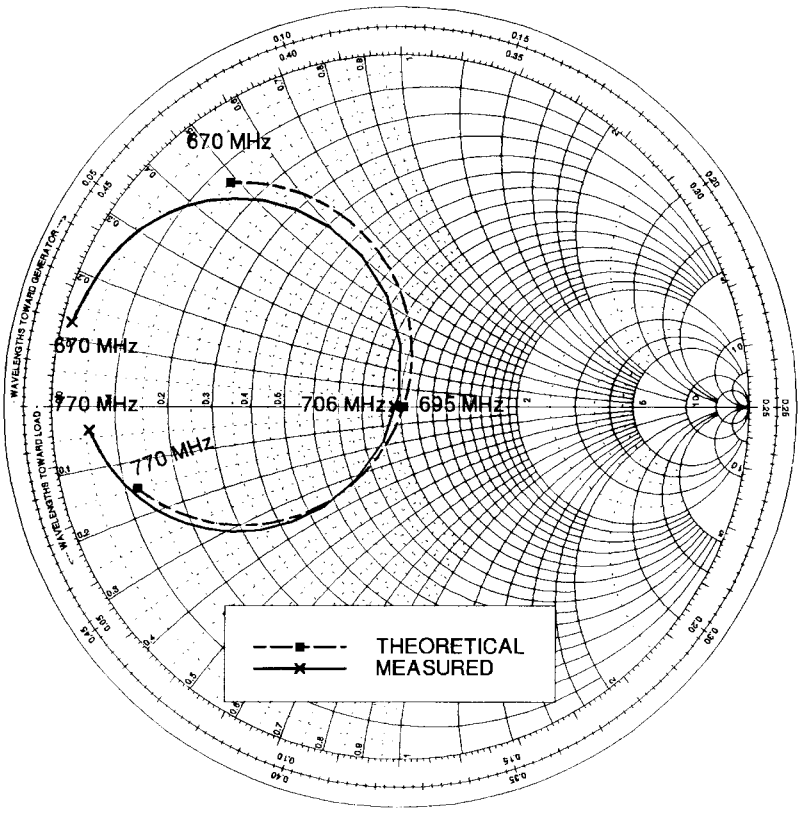

(b)

Fig. 7. (*Continued*.) Theoretical and experimental impedance loci of the antennas A, B, and C. (b) Antenna B.

For the slot S2, the aperture excitation field E_2 is given by

$$E_2 = E_0 \cos\left[\frac{n\pi}{2l_{p\,\mathrm{new}}}\left(l_{p\,\mathrm{new}} + \frac{y}{\sin\alpha}\right)\right] \quad -(l_{p\,\mathrm{new}})\sin\alpha \le y \le 0 \quad (4)$$

where

$$l_{p\,\mathrm{new}} = \left(l_p + \frac{h}{2}\right)$$

m, n are the mode numbers and E_0 is the maximum amplitude of aperture excitation. Similar expressions with appropriate limits can be used for representing the aperture excitations corresponding to S3, S5 and S6.

The far-field components produced by these aperture excitations are determined by taking their spatial Fourier transforms [13] as follows:

$$\mathcal{F}(E_a) = \int_{x_{\min}}^{x_{\max}} \int_{y_{\min}}^{y_{\max}} E_a e^{jk_x x} e^{jk_y y}\, dx\, dy \quad (5)$$

where

$$k_x = k_0 \sin\theta\cos\phi$$
$$k_y = k_0 \sin\theta\sin\phi$$
$$k_0 = \frac{2\pi}{\lambda_0} \quad \lambda_0 \text{ is the free-space wave length.}$$

The slot excitation field E_a and the limits of integration varies according to the radiating slots.

For TM_{01} mode, the far-field contributions from E_1 and E_4 have only Y-directed components and those of E_2, E_3, E_5, and E_6 have both X and Y-directed components. The total X-directed (E_x) and Y-directed (E_y) components are given by

$$\begin{aligned} E_x &= E_{3xf} e^{jk_x s_{3x}} e^{jk_y s_{3y}} + E_{6xf} e^{jk_x s_{6x}} e^{jk_y s_{6y}} \\ &\quad - E_{2xf} e^{jk_x s_{2x}} e^{jk_y s_{2y}} - E_{5xf} e^{jk_x s_{5x}} e^{jk_y s_{5y}} \\ E_y &= E_{1f} e^{jk_x s_{1x}} e^{jk_y s_{1y}} + E_{4f} e^{jk_x s_{4x}} e^{jk_y s_{4y}} \\ &\quad - E_{2yf} e^{jk_x s_{2x}} e^{jk_y s_{2y}} - E_{3yf} e^{jk_x s_{3x}} e^{jk_y s_{3y}} \\ &\quad - E_{5yf} e^{jk_x s_{5x}} e^{jk_y s_{5y}} - E_{6yf} e^{jk_x s_{6x}} e^{jk_y s_{6y}}. \end{aligned} \quad (6)$$

E_{1f} and E_{4f} are the Y-directed far-field components produced by slot excitations E_1 and E_4, respectively. E_{2xf}, E_{3xf}, E_{5xf}, and E_{6xf} are the X-directed far-field components produced due to aperture excitations E_2, E_3, E_5, and E_6, respectively. E_{2yf}, E_{3yf}, E_{5yf}, and E_{6yf} are the corresponding Y-directed far-field components. (S_{1x}, S_{1y}), (S_{2x}, S_{2y}), $\cdots$, (S_{6x}, S_{6y}) are the coordinates of the center points of the slots S1, S2, $\cdots$, S6, respectively. The total far field produced can be obtained as in [13].

The experimental and theoretical radiation patterns of the antenna configuration in Fig. 3(a) in the two principal planes are shown in Fig. 6. The cross polarization patterns of the antenna in both the planes are measured and also plotted in Fig. 6. The other two antennas (B and C) behave in a similar manner.

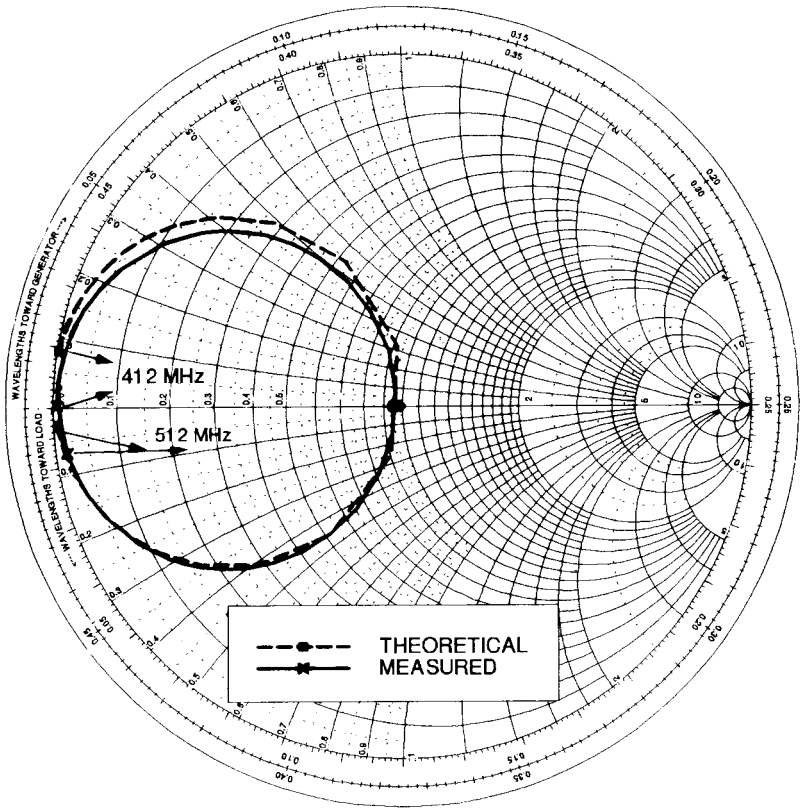

(c)

Fig. 7. (*Continued*.) Theoretical and experimental impedance loci of the antennas A, B, and C. (c) Antenna C.

The total radiated power (P_r) is computed by [13] and can be used for the calculation of quality factor and gain. The predicted and measured gain of antenna A is found to be 6.04 dB and 5.86 dB, respectively.

The total stored energy under the cavity (W_{stotal}) is determined [1] by adding the time-averaged electric and magnetic field energy under each segment and is given by

$$W_{\text{stotal}} = W_{\text{rect}} + 4W_{\text{triangle}} \tag{7}$$

where W_{rect} and W_{triangle} are the stored energy under the rectangular and triangular segments, respectively.

Here stored energy under all the segments are computed by using the same subroutine. This method does not involve the integration of Green's function and, hence, is computationally more efficient. As the conductor, dielectric, and surface wave losses are not significant at low frequencies and for lower order modes, the quality factor at the operating frequency f_{01} is given by

$$Q \approx \frac{2\pi f_{01} W_{\text{stotal}}}{P_r} = \frac{1}{\delta_{\text{eff}}}. \tag{8}$$

The wave number will be modified as

$$k_{\text{eff}}^2 = k_0^2 \varepsilon_{r\text{eff}}(1 - j\delta_{\text{eff}}) \tag{9}$$

where $\varepsilon_{r\text{eff}}$ is the effective dielectric constant. The modified effective wave number will be used for the evaluation of Green's function in (1) to get the actual input impedance variation. Fig. 7(a), (b), and (c) shows the theoretical and experimental input impedance variation for the three antennas A, B, and C, respectively.

III. Conclusion

A new compact microstrip antenna suitable for array applications is analyzed for resonance frequency, radiation pattern, and input impedance. The theoretical results are validated through experimental observations. These antenna elements may find applications in large arrays, where array size is a major concern.

Acknowledgment

The authors would like to thank Prof. R. Garg, of IIT, Karagpur, India, for his helpful discussions.

References

[1] J. R. James and P. S. Hall, *Handbook of Microstrip Antennas*. Stevenage, U.K.: Peter Peregrinus, 1989; London, U.K.: IEE, 1989.
[2] K. L. Wong, C. L. Tang, and H. T. Chen, "A compact meandered circular microstrip antenna with a shorting pin," *Microwave Opt. Technol. Lett.*, vol. 15, no. 3, pp. 147–149, June 1997.
[3] C. L. Tang, H. T. Chen, and K. L. Wong, "Small circular microstrip antenna with dual frequency operation," *Electron. Lett.*, vol. 33, no. 13, pp. 1112–1113, June 1997.
[4] K. L. Wong and S. C. Pan, "Compact triangular microstrip antenna," *Electron. Lett.*, vol. 33, no. 6, pp. 433–434, Mar. 1997.
[5] K. L. Wong and W. S. Chen, "Compact microstrip antenna with dual frequency operation," *Electron. Lett.*, vol. 33, no. 8, pp. 646–647, Apr. 1997.
[6] R. Waterhouse, "Small microstrip patch antenna," *Electron. Lett.*, vol. 31, no. 8, pp. 604–605, Apr. 1995.

[7] J. George, M. Deepukumar, C. K. Aanandan, P. Mohanan, and K. G. Nair, "New compact microstrip antenna," *Electron. Lett.*, vol. 32, no. 6, pp. 508–509, Mar. 1996.
[8] A. K. Bhattacharyya and R. Garg, "A generalized transmission line model for microstrip patches," *Proc. Inst. Elect. Eng.*, vol. 132, pt. H, no. 132, pp. 93–98, Apr. 1985.
[9] W. F. Richards, Y. T. Lo, and D. D. Harrison, "An improved theory for microstrip antennas and applications," *IEEE Trans. Antennas Propagat.*, vol. AP-29, pp. 38–46, Jan. 1981.
[10] P. Silvester, "Finite-element analysis of planar microwave networks," *IEEE Trans. Microwave Theory Tech.*, vol. MTT-21, pp. 104–108, Feb. 1973.
[11] A. Reineix and B. Jecko, "Analysis of microstrip patch antennas using finite difference time domain method," *IEEE Trans. Antennas Propagat.*, vol. 37, pp. 1361–1369, Nov. 1989.
[12] V. Palanisamy and R. Garg, "Analysis of arbitrary shaped microstrip patch antennas using segmentation technique and cavity model," *IEEE Trans. Antennas Propagat.*, vol. AP-34, pp. 1208–1213, Oct. 1986.
[13] P. Hammer, D. V. Bouchaute, D. Verschraeven, and A. V. D. Capelle, "A model for calculating the radiation field of microstrip antennas," *IEEE Trans. Antennas Propagat.*, vol. AP-27, pp. 267–270, Mar. 1979.
[14] T. Okoshi and T. Miyoshi, "The planar circuit—An approach to microwave integrated circuitry," *IEEE Trans. Microwave Theory Tech.*, vol. MTT-20, pp. 245–252, Apr. 1972.
[15] R. Chadha and K. C. Gupta, "Green's functions for triangular segments in planar microwave circuits," *IEEE Trans. Microwave Theory Tech.*, vol. MTT-28, pp. 1139–1143, Oct. 1980.
[16] K. C. Gupta, R. Garg, and R. Chadha, *Computer Aided Design of Microwave Circuits*. Norwood, MA: Artech House, 1981.
[17] T. Miyoshi and S. Miyauchi, "The design of planar circulators for wideband operation," *IEEE Trans. Microwave Theory Tech.*, vol. MTT-28, pp. 210–214, Mar. 1980.

Jacob George was born in Kerala, India, on February 20, 1970. He received the B.Sc. degree in physical science from Mahatma Gandhi University, Kerala, India, and the M.Sc. degree in electronics from Cochin University of Science and Technology (CUSAT), Cochin, India (with first rank and distinction), in 1990 and 1993, respectively. He is currently working toward the Ph.D. degree from CUSAT.

He qualified the national eligibility test (UGC-NET) for a research fellowship and lectureship in 1996. Currently, he is working as Senior Research Fellow of Council of Scientific and Industrial Research (CSIR), Government of India. His current research interests include microstrip antennas and computational electromagnetics.

C. K. Aanandan was born in India in 1959. He received the M.Sc. and Ph.D. degrees from Cochin University of Science and Technology (CUSAT), Cochin, India, in 1981 and 1987, respectively.

In 1987 he joined the Government Brennen College, Tellichery, India, as a Lecturer in physics,. Since 1990 he has been working as a Lecturer in the Department of Electronics of CUSAT. From 1997 to 1998 he worked at the Centro Studi Propagazione e Antenne, Consiglio Nazionale delle Ricerche, Torino under the TRIL programme of the International Centre for Theoretical Physics (ICTP), Trieste, Italy, where he is currently an associate member. His research interests include microstrip antennas, radar cross section studies, and frequency selective surfaces.

P. Mohanan was born India in 1956. He received the Ph.D. degree in microwave antennas from Cochin University of Science and Technology (CUSAT), Cochin, India, in 1985.

From 1980 to 1986, he worked as a Lecturer in physics at St. Albert's College, Ernakulam, India. He spent two years as in Bharat Electronics (BEL), Ghaziabad, India, as an Engineer in the Antenna Research and Development Laboratory. Since 1989 he has been working as Reader in Department of Electronics, CUSAT. His current areas of research activities include microstrip antennas, dielectric resonator antennas, superconducting microwave antennas, leaky-wave antennas, reduction of radar cross section, microwave instrumentation, etc. He has been involved in the implementation of different scientific research projects including AICTE, UGC, DOE, and MHRD.

Dr. Mohanan received the Career Award from University Grants Commission (UGC) in Engineering and Technology, Government of India, in 1994.

K. G. Nair (M'76–SM'80) was born in India. He received the M.Sc. degree in physics (specialization in electronics) and the Ph.D. degree in microwave antennas, both from the University of Kerala, in 1958 and 1966 respectively.

From 1962 to 1965, he was a Research Assistant in Council if Scientific and Industrial Ionospheric Research Unit, Trivandrum, India. In 1965 he joined as Lecturer at Delhi University (HR College), India. Later, he joined Kerala University, India, as Lecturer in physics. In 1972 he joined the Physics Department, Cochin University of Science and Technology (CUSAT), Cochin, India, as Lecturer and Reader. From 1975 to 1976, he was with the Electronics Engineering Department, University of Leeds, U.K., as a Commonwealth Academic Research Fellow. From 1980 to 1995 he worked as Professor and Head of the Department of Electronics of CUSAT, where he became Dean of Faculty of Technology and a member of Syndicate of the University. He is currently working as the Director of the newly established Sophisticated Test and Instrumentation Centre (STIC), a joint venture of CUSAT and the Government of Kerala. He is also an Emeritus Professor in the Department of Electronics of CUSAT. His research interests include microwave antennas, particularly electromagnetic horns, microstrip antennas, leaky-wave antennas, Nondestructive Testing using microwaves and radar cross section studies.

Dr. Nair is a Fellow of the Institution of Electronics and Telecommunication Engineers (India) and a Life Member of the Indian Society for Technical Education. He was nominated as the Expert Member of various committees by University Grants commission (UGC) and Union Public Service Commission (UPSC), India. In 1989 he was the recipient of the Best Paper Award of the NDT society of India and in 1992 he received the Homi J. Bhabha Award for Research in Applied Sciences from the Hari Om Ashram Trust through the UGC.